JOURNAL OF AIRCRAFT
Vol. 43, No. 6, November–December 2006

# Engineering Notes

*ENGINEERING NOTES are short manuscripts describing new developments or important results of a preliminary nature. These Notes should not exceed 2500 words (where a figure or table counts as 200 words). Following informal review by the Editors, they may be published within a few months of the date of receipt. Style requirements are the same as for regular contributions (see inside back cover).*

## Numerical Simulation of Helicopter Engine Jet and Fuselage Temperature Field

Yihua Cao,* Yuan Su,† and Qiang Zhang‡
*Beijing University of Aeronautics and Astronautics, 100083 Beijing, People's Republic of China*

DOI: 10.2514/1.25697

### Introduction

THE modern helicopters mostly employ turboshaft engine. This engine jet has characteristics of high temperature and velocity. Thus, an insight into the influence of engine jet upon helicopter structure, especially its temperature distribution, is of importance to understand the infrared radiation performance of helicopters.

As for rotor vortex flow or engine jet, some relative researches were conducted in the past. Affes and Conlisk [1,2] investigated the interaction of a rotor tip vortex with an airframe through an experimental and analytical study. Norton and Kingsley [3] made a prediction of a high bypass ratio engine exhaust nozzle flowfield. Ebrahimi and Kawasaki [4] executed a simulation of radiative heat-transfer effects from the rocket engine exhaust and they used a flowfield model to simulate the flow processes contributing to the radiative heating. Birckelbaw and Nelson [5] investigated the engine exhaust flow field about several V/STOL aircraft and the resulting heating of the aircraft and runway surfaces. Loka et al. [6] used computational fluid dynamics (CFD) to optimize the shape of turboshaft and turboprop exhausts as part of the engine development cycle. Their investigation contains a simultaneous viscous analysis of the external and internal flowfields. Griffin et al. [7] designed a new experimental facility to study the flows in turboshaft exhausts and measured the temperature field in the nozzle of the test section.

According to these previous literatures, the studies about the interaction of a rotor tip vortex with an airframe have been conducted by some researchers whereas the other researchers have investigated the temperature field of the external and internal flows of the engine. However, the coupled helicopter rotor/fuselage/engine jet flow (the coupling among the rotor, fuselage, and engine jet) is not considered. At present, few papers on the coupled helicopter rotor/fuselage/engine jet flow could be found.

In this paper, we believe that engine jet is not isolated, but it is subjected to the interference of rotor downwash and sidewash when a helicopter is in some flight states. This is a problem of an investigation into the effect of rotor crossflow on engine jet. The key to solve this problem lies in two points: 1) to make sure to know the path of the jet centerline and its velocity distribution, and 2) to calculate the jet cross section shape at different positions.

As for the first point, based on the generalized wake model, the calculation and analysis of the rotor free wake are carried out while the effect of tip vortex core on the self-induced velocity is introduced. Going on the premise of circulation convergence and wake convergence, rotor thrust is calculated until it satisfies the thrust criterion. At last, the calculations of the helicopter rotor downwash and sidewash velocity are carried out around the fuselage and engine jet space.

After the downwash and sidewash velocity distribution along the centerline of the engine jet is obtained, we can calculate the path of the jet centerline by numerical integration. As for the jet cross section shape, it is changed continuously along with the development of the jet under the effect of the crossflow shear. Usually it is calculated through using the method of setting vortices at the jet cross section boundary. Finally the convection temperature and radiation temperature are calculated for an insight into temperature distribution of a helicopter fuselage.

### Rotor Wake Analysis Model

The tip vortex location can be well simulated by a series of linear and exponential functions. For a hovering ( $\mu = 0.0$) rotor, the prescribed and generalized wake can be expressed by the following expression [8]:

Tip vortex axial coordinates and radial coordinates are, respectively,

$$Z = \begin{cases} k_1 \Psi_w & 0 \le \psi_w \le 2\pi/N_b \\ k_1(2\pi/N_b) + k_2(\Psi_w - 2\pi/N_b) & \psi_w \ge 2\pi/N_b \end{cases} \quad (1)$$

$$r = A + (1 - A)e^{-\lambda \Psi_w} \quad (2)$$

Vortex sheet axial coordinate is

$$Z = Z_{r=0} + r(Z_{r=1} - Z_{r=0}) \quad (3)$$

where

$$Z_{r=1} = \begin{cases} k_{11}\psi_w & 0 \le \psi_w \le 2\pi/N_b \\ k_{11}(2\pi/N_b) + k_{21}(\psi_w - 2\pi/N_b) & \psi_w \ge 2\pi/N_b \end{cases}$$

$$Z_{r=0} = \begin{cases} 0 & 0 \le \psi_w \le \pi/2 \\ k_{20}(\psi_w - 2\pi/N_b) & \psi_w > \pi/2 \end{cases}$$

Inner vortex sheet radial coordinate is

$$r = r_C \cdot r_B / r_D \quad (4)$$

In cylindrical polar coordinates, new wake geometry coordinates can be defined as

Received 6 June 2006; revision received 26 August 2006; accepted for publication 1 October 2006. 

*Professor, Department of Flight Vehicle Design and Applied Mechanics; yihuacs@yahoo.com.cn (corresponding author).
†Associate Professor, Department of Flight Vehicle Design and Applied Mechanics.
‡Doctoral Candidate, Department of Flight Vehicle Design and Applied Mechanics.

$$\left.\begin{array}{c}\psi_{(i+1)}^{\text{new}} = \psi_{(i)}^{\text{old}} + v(i)\Delta t/r(i) \\ r_{(i+1)}^{\text{new}} = r_{(i)}^{\text{old}} + u(i)\Delta t \\ z_{(i+1)}^{\text{new}} = z_{(i)}^{\text{old}} + w(i)\Delta t\end{array}\right\} \tag{5}$$

The circulation convergence criterion can be described as

$$\delta = \sum_{i=1}^{\text{Ne}} (\Gamma_{(i)}^{\text{new}} - \Gamma_{(i)}^{\text{old}})^2 \Big/ \sum_{i=1}^{\text{Ne}} (\Gamma_{(i)}^{\text{new}})^2 \le \delta_0 \tag{6}$$

where $\delta_0$ can be generally taken as $\delta_0 = 5.0 \times 10^{-5}$, and its selection depends on the compromise between the calculating time and accuracy requirement.

As for the downwash velocity field, using the Biot–Savart Law based on geometry results, the downwash velocity induced by bound vortex and trailing vortices for any point can be calculated [9,10].

## Engine Jet/Rotor Downwash Analysis Method

Theoretically, the engine jet of a helicopter is subjected to the interference of the rotor downwash [11]. For convenience, let

$$\begin{gathered} U_\infty = W\cos\theta; \qquad V_\infty = -W\sin\theta; \qquad \bar{y}_e = y_e/y_{eo} \\ \bar{U} = U/U_o; \qquad \bar{V} = V/V_o; \qquad \bar{W} = W/W_o; \qquad \bar{T} = T/T_o \\ \bar{\rho} = \rho/\rho_\infty \end{gathered} \tag{7}$$

thus the elementary equations for the jet calculation are as follows.

### Momentum Equation in Centerline Direction

$$A\frac{\mathrm{d}p_j}{\mathrm{d}z_l} + \frac{\mathrm{d}}{\mathrm{d}z_l}\int_A \rho U^2\,\mathrm{d}A = \rho_\infty E U_\infty \tag{8}$$

where $E$ is the volumetric entrainment rate, which is defined as

$$E = \frac{1}{\rho}\frac{\mathrm{d}}{\mathrm{d}z_l}\int_A \rho U\,\mathrm{d}A \tag{9}$$

### Momentum Equation in Direction Normal to the Centerline

$$A\frac{\mathrm{d}p_j}{\mathrm{d}z_l} = -\frac{1}{2}\rho_\infty A U_\infty \frac{\mathrm{d}U_\infty}{\mathrm{d}z_l} \tag{10}$$

### Momentum Relation in Direction Normal to the Jet

The preceding equations can be used to derive the momentum relation in direction normal to the jet. The result is

$$C_D y_e V_\infty^2 + \left(\frac{\mathrm{d}\theta}{\mathrm{d}z_l}\right)\int_A \bar{\rho}U^2\,\mathrm{d}A = V_\infty \frac{\mathrm{d}}{\mathrm{d}z_l}\int_A \bar{\rho}U\,\mathrm{d}A \tag{11}$$

The expansion rate equation of the jet cross section [12]

$$\frac{\mathrm{d}A}{\mathrm{d}z_l} = \frac{2\sqrt{\pi A}}{U_m}\left[G(U_m - U_\infty) - \frac{\alpha K_1 V_\infty}{(A_o/A_1)^{(1-A_1)/2} + K_2}\right] \tag{12}$$

where

$$\begin{gathered} \mathrm{G} = 0.22, \qquad \alpha\mathrm{K}_1 = 0.38, \qquad \mathrm{K}_2 = 0.50 \\ A_1 = \frac{\exp[z_l V_{\infty o}/\pi y_{eo}]}{6.2\bar{W}}, \qquad \bar{V}_{\infty o} = -W\sin\theta_o/U_o = -\bar{W}\sin\theta_o \end{gathered} \tag{13}$$

### Excess Enthalpy Equation

$$\int_A \rho u(T - T_\infty)\,\mathrm{d}A = \rho_0 u_0 (T_0 - T_\infty) A_0 \tag{14}$$

### Cross Section Constant Distribution Expressions in the Main Segment of Jet

$$\left.\begin{array}{c}\frac{u}{u_m} = (1 - \xi^{3/2})^2 \\ \frac{T - T_\infty}{T_m - T_\infty} = 1 - \xi^{3/2} \\ \xi = y/y_e\end{array}\right\} \tag{15}$$

where $y_e$, $T_m$, $U_m$, $\theta$ are unknown quantities in the main segment. If the calculated downwash velocity is taken as boundary condition, the preceding equations can be used to solve $y_e$, $T_m$, $U_m$, $\theta$ in any cross sections of the jet.

### Calculation of the Jet Cross Section Shape

The effect of the crossflow on the jet cross section can be calculated by adopting the method of setting even vortices around the outlet cross section of the jet. The induced velocity of these vortices can be calculated via the following expression:

$$\begin{aligned} V_\eta = {} & \frac{2\Gamma_0}{\pi}\sum_{n=1}^{N}\sin\left[\frac{2\pi}{N}(n-1)\right] \\ & \times \frac{(\xi - \xi_n)(1 - \exp\{[(\eta - \eta_n)^2 + (\xi - \xi_n)^2]/(4v_l)\})}{(\eta - \eta_n)^2 + (\xi - \xi_n)^2} \end{aligned} \tag{16}$$

$$\begin{aligned} V_\xi = {} & -\frac{2\Gamma_0}{\pi}\sum_{n=1}^{N}\sin\left[\frac{2\pi}{N}(n-1)\right] \\ & \times \frac{(\eta - \eta_n)(1 - \exp\{[(\eta - \eta_n)^2 + (\xi - \xi_n)^2]/(4v_l)\})}{(\eta - \eta_n)^2 + (\xi - \xi_n)^2} \end{aligned} \tag{17}$$

$$\Gamma_0 = W\sin(\theta) R_0 \sin(\pi/N) = \text{const.} \tag{18}$$

where $N$ is the number of vortices.

The area geometry center criterion, usually Owen arithmetic, is employed to check out to ensure the reliability of the calculation results.

## Temperature Field Calculation Method

The path of engine jet centerline changes under the effects of rotor sidewash and downwash. It can be figured out with numerical integral method.

Temperature field of a helicopter in this paper only involves two parts. One is called the convection temperature that comes from convection of engine jet. The other is called radiation temperature, coming from radiation of engine jet that can be regarded as heat source.

### Calculation of Convection Temperature

Because of rotor sidewash and downwash, engine jet encounters the fuselage. Furthermore, temperature distributions subjected to engine jet can be considered as those that consist in several temperature vortices with different temperature. When some vortices encounter several points on the fuselage, it transfers heat to these points through convection of engine jet, which causes temperature of these points to rise into the one of the vortex. The whole engine jet encounters the fuselage at many points and the temperatures of these points are equal to the vortex temperatures in engine jet. Then the convection temperature field can be calculated.

**Calculation of Radiation Temperature**

The engine jet of helicopter can be regarded as heat source with constant temperature distribution, and it radiates heat to environment continuously. Thus a steady radiant temperature field appears on the fuselage. Heat source method can be used to calculate this temperature field.

The engine jet can be divided into many segments. Each segment can be regarded as a tiny heat source. The temperature caused by a tiny heat source can be calculated with this expression:

$$\theta(D) = \frac{Q_p}{4\pi\lambda D} \tag{19}$$

In this expression, $Q_p$ is the radiant power of the tiny heat source and $\lambda$ is the coefficient of heat exchange. $D$ is the distance between tiny heat source and a point on the fuselage.

If the engine jet is divided into $m$ heat sources, the total radiant temperature of a point on the fuselage can be calculated with the following expression:

$$T_r = \sum_{i=1}^{m} \theta_i \tag{20}$$

In this expression, $\theta_i$ is the radiant temperature of this point caused by the $i$th heat source.

**Final Temperature Field on Fuselage**

The final temperature of a point on the fuselage can be calculated through adding the convection temperature and radiation temperature to environmental temperature:

$$T_f = T_\infty + T_c + T_r \tag{21}$$

In this expression, $T_\infty$, $T_c$, and $T_r$ are, respectively, environmental temperature, convection temperature, and radiation temperature. If a point on the fuselage does not encounter any temperature vortex, this expression regresses into

$$T_f = T_\infty + T_r \tag{22}$$

It should be noted that engine jet can only encounter with the points on the back body part of the fuselage because the engine spout (i.e., engine outlet) lies in the middle of fuselage. Therefore, convection temperature field only lies in the back body part of the fuselage whereas radiation temperature field lies in the whole fuselage surface.

## Calculation Results and Analysis

**Engine Jet/Rotor Downwash**

The rotor downwash velocity along the engine jet centerline at hover is calculated based on the structure data of a typical helicopter (rotor radius $R = 5.965$ m, rotor rotational speed $\Omega = 36.5472$ rad/s, see Fig. 1). Size of the helicopter, rotor, type of engine, and geometry of the engine outlets in this sample calculation are similar to those of the Dolphin 2 (SA 365N) Helicopter [13]. In Fig. 1, two coordinate systems are defined as follows. The first one is rotor construction axes system $o_sX_sY_sZ_s$. Coordinate origin $o_s$ is taken as rotor hub center. $o_sX_s$-axis aims to the longitudinal construction direction, and $o_sZ_s$ is in the vertical plane. $o_sY_s$-axis is perpendicular to $o_sX_sZ_s$ plane. It is a left-hand coordinate system.

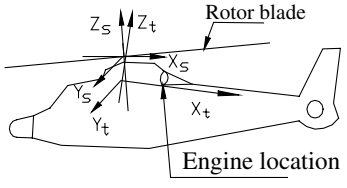


**Fig. 1 Relative location of engine.**

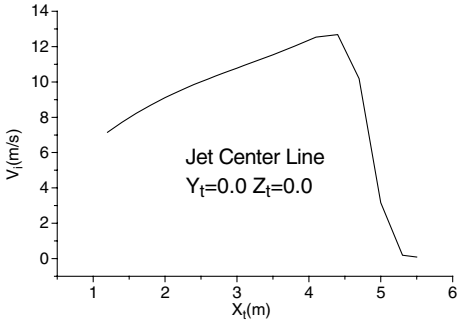


**Fig. 2 Rotor downwash velocity along the engine jet centerline.**

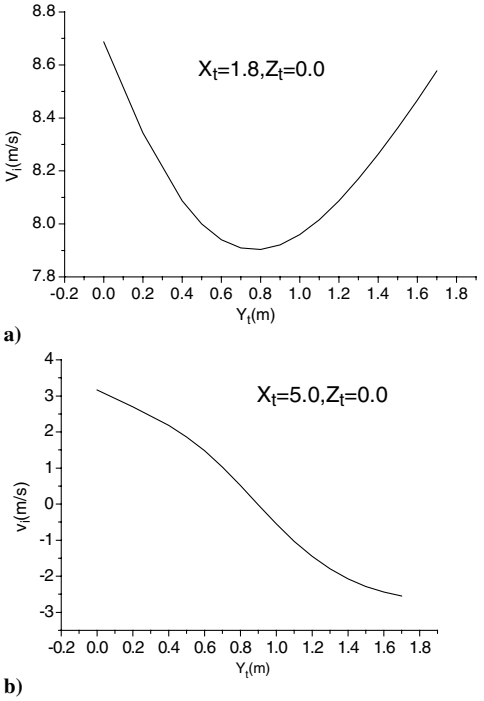


**Fig. 3 Downwash velocity distribution at discrete cross sections along the engine jet centerline.**

The second one is engine body fixed axes system $o_tX_tY_tZ_t$. $o_tX_t$ is along the engine centerline (i.e., centerline between left engine and right engine). It is also a left-hand coordinate system. Figure 2 shows the calculation results of the rotor downwash velocity along the engine jet centerline ($\mu = 0.0$). The variation trend of these results is similar to that of the computed and measured airflow velocities [14,15]. From the figures it can be found that the rotor downwash increased at first and then dropped along the engine jet centerline. For insight into the transverse distribution of rotor downwash in detail, Fig. 3 shows a typical rotor downwash velocity distribution at discrete cross sections along the engine jet centerline ($X_t = 1.8, 5.0$). From overall distribution, we can see that the downwash velocity decreases at first and then increases with the increase of $Y_t$ at the cross section $X_t = 1.8$ while the downwash velocity decreases continuously at the cross section $X_t = 5.0$.

Let us take the preceding calculated results as initial velocity boundary condition and give the following initial parameters:

1) Outlet parameters and environment parameters

$$p_\infty = 101,300 \text{ Pa}, \quad T_\infty = 20^\circ\text{C}, \quad \upsilon_\infty = 1.046 \times 10^5 \text{ m}^2/\text{s}$$
$$Q_0 = 2.5 \text{ kg/s}, \quad A_0 = 0.078179 \text{ m}^2, \quad y_{e0} = 0.1557 \text{ m}$$
$$p_0 = 102,000 \text{ Pa}$$

where $Q_0$ is flow flux, $A_0$ is area, $y_{e0}$ is equivalent radius of engine outlet area, and $p_0$ is pressure.

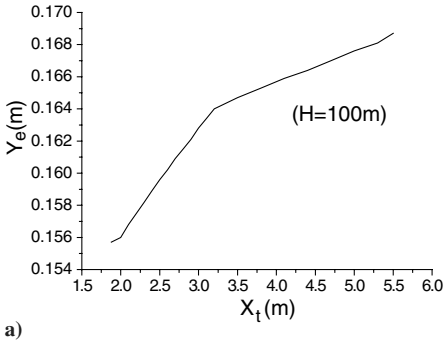


a)

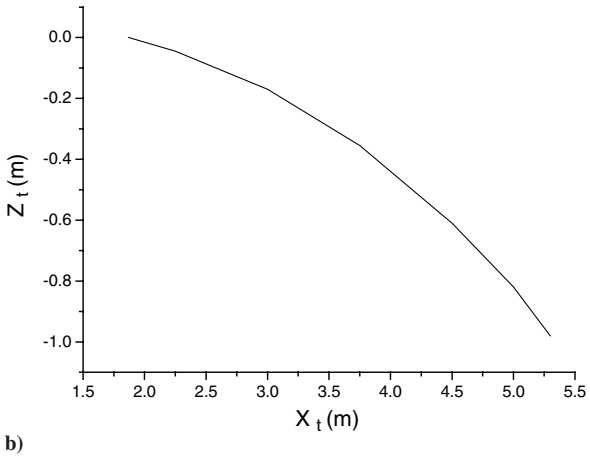


b)

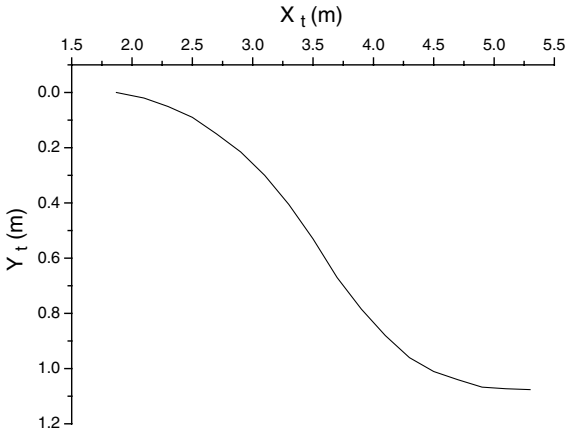


c)

**Fig. 4 a) Equivalent radius of the jet boundary; b) effect of rotor downwash on jet centerline path; c) effect of rotor sidewash on jet centerline path.**

2) Outlet geometry center coordinate and other parameters

$$X_{p0} = 1.8791 \text{ m}, \quad Y_{p0} = 0.4219 \text{ m}, \quad Z_{p0} = 0.4753 \text{ m}$$
$$H = 100.0 \text{ m}, \quad T_0 = 636.0^\circ\text{C}, \quad U_0 = 84.13 \text{ m/s}$$
$$\rho_0 = 0.38 \text{ kg/m}^3$$

3) Other initial parameters

$$Z_{L0} = 0, \quad \theta_0 = 90 \text{ deg}, \quad W_0 = W(0)$$

The calculation results and analyses are as follows: Fig. 4a shows $Y_e$–$X_t$ plot, where abscissa $X_t$ is a coordinate of cross section in engine body fixed axes system and $Y_e$ is the equivalent radius of the jet boundary. It is well known that engine jet path should be drifted under the effects of rotor downwash and sidewash. Figures 4b and 4c show, respectively, downward drift and leftward drift of the jet centerline path due to effects of rotor downwash and sidewash.

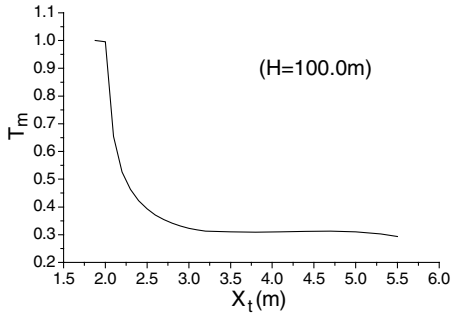


**Fig. 5 Temperature of engine jet core.**

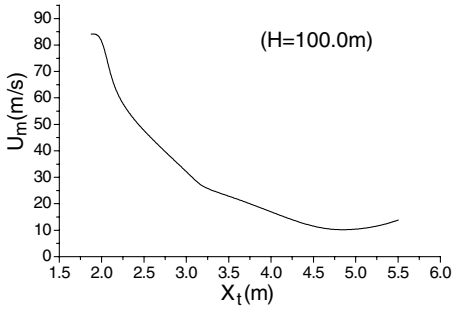


**Fig. 6 Velocity of engine jet core.**

Figure 5 is $T_m$–$X_t$ graph, where abscissa $X_t$ is a coordinate of cross section in engine body fixed axes system and $T_m$ is the temperature of the jet core. Here $T_m$ is a dimensionless result, its characteristic value for this dimensionless result is 909.15 K.

Figure 6 presents $U_m$–$X_t$ graph, where abscissa $X_t$ is a coordinate of cross section in engine body fixed axes system and $U_m$ is the velocity of the jet core. Figure 7 is vortex line distribution graph of the calculated engine jet cross section ($X_t = 2.0$ m), where $Y_p$, $Z_p$ are coordinates. In Fig. 7 $X_t$ is coordinate value of area geometry center of engine jet at a cross section in engine body fixed axes system $o_t X_t Y_t Z_t$. $Y_p$ and $Z_p$ are used to depict the setting vortex line of the engine jet. The origin of $Y_p$ and $Z_p$ is taken as the area geometry center of engine jet. The numbers shown in Fig. 7 are temperature value (°C).

**Temperature Field**

Figure 8 shows a typical helicopter three-dimensional grid system. The calculated temperature distribution of the helicopter is shown in Fig. 9.

It can be found in Fig. 9 that the rotor is not shown so that the temperature distribution can be shown more clearly, and the numbers represent different ranges of temperature that are listed in Table 1.

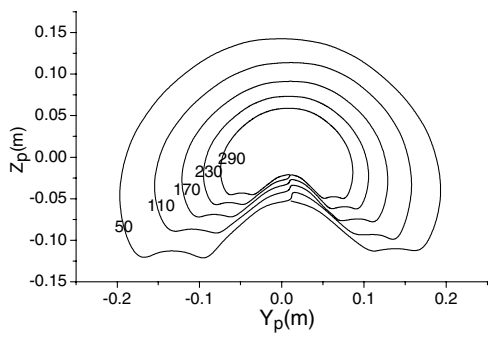


**Fig. 7 Temperature distribution of engine jet at a cross section ($X_t = 2.0$ m).**

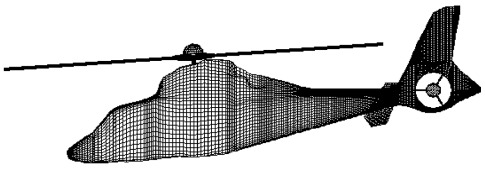

**Fig. 8 Three-dimensional grid plot of the helicopter.**

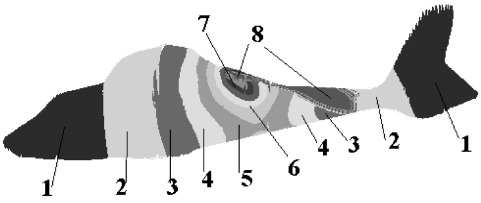


**Fig. 9 Temperature distribution of the helicopter.**

**Table 1 Corresponding relations between numbers of Fig. 9 and ranges of temperature**

| Number | Range of temperature, °C |
|---|---|
| 1 | 23–35 |
| 2 | 35–47 |
| 3 | 47–59 |
| 4 | 59–71 |
| 5 | 71–83 |
| 6 | 83–107 |
| 7 | 107–131 |
| 8 | 131–218 |

## Conclusions

This paper presents a numerical simulation method to predict helicopter engine jet and fuselage temperature field. Rotor free wake analysis was first carried out to calculate rotor wake geometry and the downwash velocity field around the engine jet space. Then engine jet path, cross section shape, and physical variants were calculated and analyzed. Finally, an engineering method was given to calculate the fuselage temperature for insight into the influence of engine jet upon the temperature distribution around a helicopter. The method established here can be used to predict rotor wake, engine jet, and temperature distribution of a helicopter.

Future work should be focused on CFD method because it has provided an effective design tool for engineering problems, particularly in problems where experimental testing is too time-consuming or expensive. Furthermore, with the development of computational techniques, and high-speed and large capacity computers, CFD (Euler/Navier–Stokes) simulations for rotor flow are being fully realized. The simulation of coupled helicopter rotor/fuselage/engine flow through CFD is well expected. Therefore, it does appear that it is an area needed to strengthen in future studies for helicopter fluid mechanics.

## References

[1] Affes, H., and Conlisk, A. T., "A Simplified Model for the Interaction of a Rotor Tip Vortex with an Airframe," AIAA Paper 92-0320, Jan. 1992.

[2] Affes, H., and Conlisk, A. T., "An Experimental and Analytical Study of the Interaction of a Vortex with an Airframe," AIAA Paper 92-0319, Jan. 1992.

[3] Norton, R. J. G., and Kingsley, J. P., "Prediction of a High Bypass Ratio Engine Exhaust Nozzle Flowfield," AIAA Paper 92-3259, July 1992.

[4] Ebrahimi, H. B., and Kawasaki, A., "Numerical Investigation of Exhaust Plume Radiative Transfer Phenomena," AIAA Paper 98-3623, July 1998.

[5] Birckelbaw, L. D., and Nelson, E. L., "Infrared Flow Visualization of V/STOL Aircraft," AIAA Paper 92-4253, July 1992.

[6] Loka, M., Robichaud, M., Di Bartolomeo, W., Loe, D., and Sowers, D., "Aerodynamic Optimization of the Exhaust-Ejector on the Tiltrotor Using Navier–Stokes Analysis," AIAA Paper 2000-0986, Jan. 2000.

[7] Griffin, D. K., Ireland, P. T., and Ponton, A. J., "High Temperature Turbine Exhaust Flow Test Facility," AIAA Paper 2000-2209, June 2000.

[8] Landgrebe, A. J., "The Wake Geometry of a Hovering Helicopter Rotor and Its Influence on Rotor Performance," *Journal of the American Helicopter Society*, Vol. 17, No. 4, 1972, pp. 3–15.

[9] Cao, Y., "A New Method for Predicting Rotor Wake Geometries and Downwash Velocity Field," *Aircraft Engineering and Aerospace Technology*, Vol. 71, No. 2, 1999, pp. 129–135.

[10] Felker, F. F., Quackenbush, T. R., Bliss, D. B., and Light, J., "Comparisons of Predicted and Measured Rotor Performance in Hover Using a New Free Wake Analysis," *Vertica*, Vol. 14, No. 3, 1990, pp. 361–383.

[11] Cao, Y., and Su, Y., "Insight into the Effects of Rotor Downwash on Engine Jet," *Aircraft Engineering and Aerospace Technology*, Vol. 75, No. 4, 2003, pp. 345–349.

[12] Adler, D., and Baron, A., "Prediction of a Three-Dimensional Circular Turbulent Jet in Crossflow," *AIAA Journal*, Vol. 17, No. 2, 1979, pp. 168–174.

[13] Prouty, R. W., *Helicopter Performance, Stability and Control*, PWS Publishing, Boston, 1986, Appendix B.

[14] Cao, Y., Yuan, K., and Li, X., "Computational Methods for the Simulation of the Flow Around Helicopter Engine Inlet," *Journal of Aircraft*, Vol. 43, No. 1, 2006, pp. 141–146.

[15] Landgrebe, A. J., Taylor, R. B., and Egolf, T. A., "Helicopter Airflow and Wake Characteristics for Low Speed and Hovering Flight," *Journal of the American Helicopter Society*, Vol. 27, No. 4, 1982, pp. 74–83.